Cell-free DNA from nail clippings as source of normal control for genomic studies in hematologic malignancies

Melissa Krystel-Whittemore,[1°] Kseniya Petrova-Drus,[1] Ryan N. Ptashkin,[1°] Mark D. Ewalt,[1] JinJuan Yao,[1] Ying Liu,[1] Menglei Zhu,[1] Jamal Benhamida,[1] Benjamin Durham,[1] Jyoti Kumar,[1] Khedoudja Nafa,[1] Iwona Kiecka,[1] Anita S. Bowman,[1] Erika Gedvilaite,[1] Jacklyn Casanova,[1] Yun-Te Lin,[1] Abhinita S. Mohanty,[1] Satshil Rana,[1] Anoop Balakrishnan Rema,[1] Ivelise Rijo,[1] Nelio Chaves,[1] Paulo Salazar,[1] Anita Yun,[1] Sean Lachhander,[1] Wei Wang,[1] Mohammad S. Haque,[1] Wenbin Xiao,[1] Mikhail Roshal,[1] Sergio Giralt,[2] Gilles Salles,[2] Raajit Rampal,[2] Eytan M. Stein,[2] Miguel-Angel Perales,[2] Steven Horwitz,[2] Ann Jakubowski,[2] Doris Ponce,[2] Alina Markova,[2] Ozge Birsoy,[1] Diana Mandelker,[1] Simon Mantha,[2] Ahmet Dogan,[1] Ryma Benayed,[1°] Marc Ladanyi,[1] Michael F. Berger,[1] A. Rose Brannon,[1] Ahmet Zehir,[1°] Chad Vanderbilt[1#] and Maria E. Arcila[1#]

[1]Department of Pathology and Laboratory Medicine and [2]Department of Medicine, Memorial Sloan Kettering Cancer Center, New York, NY, USA

[#]CV and MEA contributed equally as last authors.

[°]Current address for MK-W: Department of Pathology, NYU Langone Health, New York, NY, USA
[°]Current address for RNP: C2i Genomics, New York, NY, USA
[°]Current address for RB and AZ: Precision Medicine and Biosamples, AstraZeneca, New York, NY, USA

Correspondence: M. Arcila
arcilam@mskcc.org

Received: January 12, 2024.
Accepted: February 29, 2024.
Early view: March 7, 2024.

https://doi.org/10.3324/haematol.2024.285054

Abstract

Comprehensive genomic sequencing is becoming a critical component in the assessment of hematologic malignancies, with broad implications for patients' management. In this context, unequivocally discriminating somatic from germline events is challenging but greatly facilitated by matched analysis of tumor:normal pairs of samples. In contrast to solid tumors, in hematologic malignancies conventional sources of normal control material (peripheral blood, buccal swabs, saliva) could be highly involved by the neoplastic process, rendering them unsuitable. In this work we describe our real-world experience using cell-free DNA (cfDNA) isolated from nail clippings as an alternate source of normal control material, through the dedicated review of 2,610 tumor:nail pairs comprehensively sequenced by MSK-IMPACT-heme. Overall, we found that nail cfDNA is a robust germline control for paired genomic studies. In a subset of patients, nail DNA may be contaminated by tumor DNA, reflecting unique attributes of the hematologic disease and transplant history. Contamination is generally low level, but significantly more common among patients with myeloid neoplasms (20.5%; 304/1,482) than among those with lymphoid diseases (5.4%; 61/1,128) and particularly enriched in myeloproliferative neoplasms with marked myelofibrosis. When identified in patients with lymphoid and plasma-cell neoplasms, mutations commonly reflected a myeloid profile and correlated with a concurrent/evolving clonal myeloid neoplasm. Donor DNA was identified in 22% (11/50) of nails collected after allogeneic stem-cell transplantation. In this cohort, an association with a recent history of graft-*versus*-host disease was identified. These findings should be considered as a potential limitation to the use of nails as a source of normal control DNA but could also provide important diagnostic information regarding the disease process.

Introduction

Hematologic malignancies constitute a diverse set of primarily myeloid and lymphoid neoplasms characterized by somatically acquired genetic alterations which promote cell survival and proliferation. Today, genetic characterization is a pivotal component of nearly every form of hematologic malignancy, with increasing roles in diagnosis, classification, prognostication, therapeutic decision-making and monitoring.

Due to the complexity and broad range of genetic alterations that may define each disease, next-generation sequencing (NGS) has emerged as a more practical approach for upfront comprehensive assessment over existing low-throughput

techniques. An inherent challenge of such studies lies in the ability to correctly distinguish somatically acquired (cancer specific) from germline alterations when using a tumor-only model. Paired studies, matching tumor and normal samples, constitute a superior method that allows unequivocal determinations and enables more sophisticated and accurate analyses of genetic variants.

Blood, buccal swabs, and saliva are traditional sources of normal control DNA for paired sequencing in solid tumors. Depending on the hematologic malignancy, however, these controls are unsuitable because of the presence of neoplastic cells at various levels. Nail clippings are an alternative source but their use in routine clinical practice has not been sufficiently explored.

In this study, we describe our experience using DNA derived from nail tissue. We describe our rapid protocol for extraction, performance characteristics and overall results based on the routine clinical sequencing of 2,610 tumor:nail pairs with our hybrid capture MSK-IMPACT-heme assay (Memorial Sloan Kettering Integrated Mutation Profiling of Actionable Cancer Targets for Hematologic malignancies). We further discuss the benefits and pitfalls and highlight unique findings using this tissue source.

Methods

Diagnostic tumor samples (blood, bone marrow, tumor biopsies) submitted for routine molecular profiling using MSK-IMPACT-heme were selected, specifically those submitted with nails as the normal control. Fingernail clippings were submitted following standard nail collection protocols described in the *Online Supplementary Methods* section. All patients provided informed consent for paired sequencing and the study was conducted following Memorial Sloan Kettering Institutional Review Board approval. Relevant clinicopathological information was retrieved from the patients' electronic medical records. Each diagnosis was confirmed by a board-certified hematopathologist and a molecular pathologist.

Sample preparation

Tumor DNA was extracted using previously described protocols.[1] Nail DNA extraction was performed using a QIAamp® DNA investigator kit (Qiagen) for forensic and human identity samples. Two nail fragmentation methods were used (Figure 1A). Method 1 followed the manufacturer's protocol strictly. Briefly, nail clippings (2-3, ~10 mg) were cut into 1-2 mm fragments with scissors before overnight digestion in proteinase K. When undigested particles were present after overnight incubation, additional proteinase K was added, and the process was repeated for several cycles to allow complete digestion. In method 2, nail clippings (~10 mg) were pulverized using a BeadBlaster™ tissue homogenizer (Benchmark Scientific, NJ, USA) following adjusted bone tissue protocols,[2,3] detailed in the *Online Supplementary Methods* section. Method 1 was used clinically from January 2017 to June 2019 and method 2 from July 2019 to December 2021.

DNA concentration was measured by a Qubit fluorometer using the dsDNA HS Assay kit (ThermoFisher Scientific/Invitrogen Cat. N. QC32854). Subsets were analyzed by the Agilent 5300 Fragment Analyzer System with the HS Small Fragment kit and the HS Genomic DNA kit (Agilent, Santa Clara, CA, USA) to assess fragment profiles, following the manufacturers' protocols.

Sequencing and data analysis

Sequencing was performed by MSK-IMPACT-heme, a custom hybridization capture-based NGS assay for the detection of somatic mutations and copy number alterations in coding regions of 400 genes.[1] Library preparation, sequencing, variant calling, and annotation were performed using matched tumor:normal pair analysis pipelines as previously described.[1,4-6] Donor DNA was also sequenced as a normal control in post-transplant cases. Variant calling was performed in paired-sample mode with manual curation, side-by-side with the corresponding results of the nail and donor samples (when applicable), at the same position. Final variant calling was performed in the context of the patient's clinicopathological history, incorporating information on annotated population frequencies, when necessary. When available, correlation with prior and subsequent samples was performed.

Analysis of nail sequencing results

Somatic variants clinically reported in tumor samples were extracted from the database along with the variant allele frequencies (VAF) of the same alterations in the nail sample. Accompanying metadata were extracted, including depth of coverage at the variant start site, OncoKB classification,[7] and variant class (indel, single nucleotide variant, etc.). Nail mutations were called if the variant was detected at a VAF of ≥1% with at least five supporting reads. Any alteration below this level was within our established level of noise for the assay and were filtered out.

Statistics

Statistical analysis was performed using R (version 4.1.1). Variables were analyzed using both paired and unpaired *t* tests, as applicable.

Results

Extraction

A side-by-side comparison of the two methods was performed on a validation set (20 samples). Overall, method 2 had a markedly shorter procedural time and improved yields. Method 1 required several digestion cycles (2-6

days), compared to a single digestion cycle for method 2 (overnight). Mean DNA yields averaged 12.5 ng/mg and 20.9 ng/mg (1.7-fold increase) for methods 1 and 2, respectively. DNA fragment sizes were compared to determine the effect of mechanical pulverization. Using the 5300 Fragment Analyzer System with the HS Small Fragment kit, the average fragment length was 154 bp and 169 bp for methods 1 and 2, respectively (Figure 1B); the differences were not statistically significant as determined by a paired *t* test (*P*=0.16). To further assess for the presence of larger fragments, a

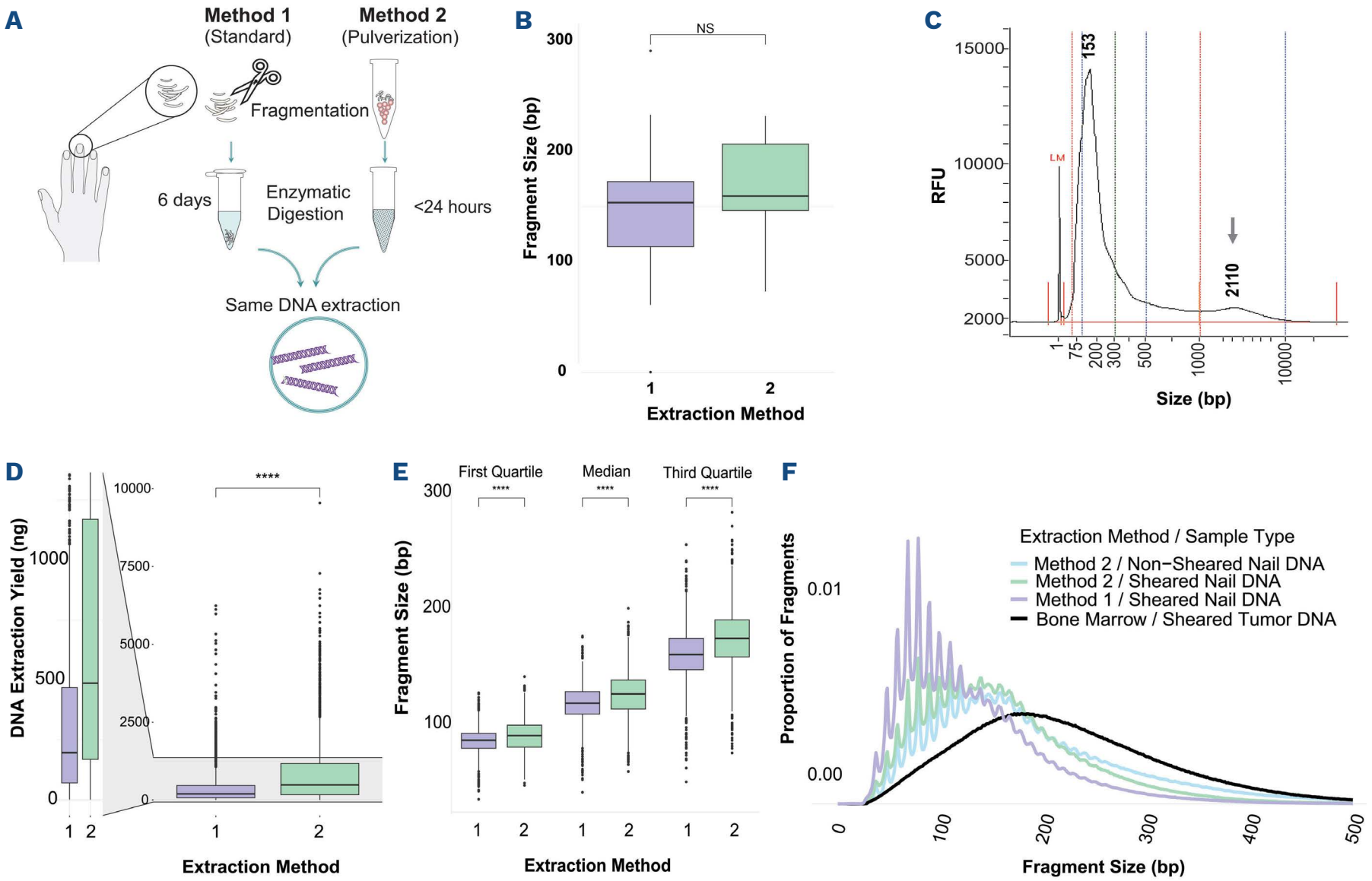

Figure 1. Summary of extraction methods and DNA quality characteristics. (A) Description of the two nail processing methods. Nail clippings were manually cut with scissors into small fragments (method 1) or pulverized (method 2), followed by enzymatic digestion and DNA extraction. Processing by method 1 takes several days for digestion (up to 6 days) whereas method 2 is much quicker (<24 hours, generally overnight). (B) Comparison of fragment sizes obtained from methods 1 and 2 established using the 5300 Fragment Analyzer System with the HS Small Fragment kit. The average sizes were 154 bp and 169 bp for methods 1 and 2, respectively. The difference was not statistically significant (*P*=0.16). (C) Representative electropherogram showing the DNA fragment distribution obtained from a nail sample analyzed by the Agilent 5300 Fragment Analyzer System with the HS Genomic DNA kit. DNA is primarily composed of short fragments with a main peak centered around 150 bp; highest point at 153 bp. Note that the high molecular weight DNA (arrow) present represents a minimal proportion of the total DNA. The numbers across the x and y axis are relabeled with larger characters over the original electropherogram to facilitate viewing. (D) Comparison of total DNA yields in nanograms (ng) observed across 4,356 nail DNA examples extracted between January 2017 and December 2021, stratified by method type; 1,807 and 2,616 were processed by methods 1 and 2, respectively. Average total DNA yields (Qubit measurements) were significantly lower for method 1, 398.7 ng (minimum: 1.3, median: 184.8, maximum: 6,240.0), compared to method 2, 835.4 ng (minimum: 1.2, median: 470.4, maximum: 9,540.0). The method is labeled on the x axis and total DNA yield denoted on the y axis. The overall distribution for methods 1 and 2 is depicted on the right and zoomed details are shown on the left. Differences are statistically significant ($P<2.2x10^{-16}$). (E) Comparison of insert sizes from sequenced libraries (sheared) of samples processed with the two methods. Insert sizes for each sample were divided by size and stratified into quartiles. Overall, samples processed by method 1 had a higher proportion of shorter inserts with statistically significant differences (*P*<0.001) as compared to samples processed with method 2, suggesting greater degradation. Method 1 (mean 118 bp, range 41-176, standard deviation 17.6) compared to method 2 (mean 126, range 59-200, standard deviation 20.0) (F) Representative insert distribution plot including several clinical samples. Library insert sizes are shown on the x axis and density (proportion of total) on the y axis. Note that nail DNA exhibits a prominent jagged or sawtooth pattern with 10 bp periodicity in fragments below 150 bp. This is seen across all nail samples (sheared and non-sheared) but is most prominent in samples processed with method 1 after several days of digestion, in contrast to the pattern observed on sheared bone marrow DNA. Source data are provided as a Source Data file. **** denotes statistically significant differences. bp: base pairs; NS: no statistical significance; RFU: relative fluorescence unit.

set of 17 samples processed with method 2 were randomly selected for analysis using the HS Genomic DNA kit. In all cases, the dominant peak was observed to migrate between the 75 and 163 bp range, at a modal length of 153 bp. The variable presence of second and/or third minor peaks was also observed, averaging 672 and 2,021 bp (migration range ~550-900 and ~900-7,000, respectively). A representative electropherogram is presented in Figure 1C.

Clinical cohort

Between January 2017 and December 2021, 4,395 nail samples were received for extraction of DNA: 1,807 and 2,616 were processed by methods 1 and 2, respectively (including 28 processed by both methods corresponding to the validation set and 8 samples repeated during method transition). For clinical testing, DNA was routinely extracted from two or three clippings without weight measurements. Total DNA yield was significantly lower with method 1 than with method 2 (average 398.7 ng *vs.* 835.4 ng, respectively; $P<2.2x10^{-16}$) (Figure 1D). At initial extraction, 79.5% (1,438/1,807) and 89% (2,329/2,616) of samples extracted with methods 1 and 2, respectively, met the minimum optimal input for sequencing by our assay (50 ng). Re-extraction of 83 samples with higher input rescued 68.7% (61.5%; 32/52 method 1 and 80.6%; 25/31 method 2).

Sequencing data

In total, 2,610 unique tumor:normal pairs of samples (2,610 patients) were sequenced for initial characterization. Monitoring tumor samples from the same patient were excluded to avoid duplication. The median interval for collection of the nail and tumor samples was 3 days (average 42 days; range, -1,512 days to +7,042 days); 88% of nail clippings were collected within ±120 days of the tumor sampling. Outliers were related to retrospective sequencing of a remote tumor or use of an archived nail sample (*Online Supplementary Table S1*).

For nail samples, insert size distributions were significantly shorter for those processed with method 1, as detailed in Figure 1E. Mean targeted coverages were also lower, averaging 785X (range, 100-1,484, median 805, standard deviation 245) for method 1, *versus* 948X for method 2 (range, 126-2,742, median 939, standard deviation 312.2) ($P<2.2x10^{-16}$). The typical insert size distribution and pattern of nails are shown in Figure 1F.

In all, 10,942 somatic mutations were detected across tumors (4,640 and 6,302 in myeloid and lymphoid disease categories, respectively). Of these, 792 (7.2%) were detected in the corresponding nails of 365 patients (13.9%; 365/2,610). Mutations in nail DNA were significantly more common among patients with myeloid neoplasms (20.5%; 304/1,482) than in those with lymphoid diseases (5.4%; 61/1,128) ($P<2.2x10^{-16}$). The overall distribution of patients, according to broad disease categories, is presented in Figure 2A, B, and *Online Supplementary Table S2*. The average number of mutations per nail was two (range, 1-12).

To further establish general trends, mutations were stratified by VAF (Figure 2C). The average tumor VAF was 26.7% (range, 1-99.7%); if present, nail mutations were detected at a significantly lower level ($P<2.2x10^{-16}$), averaging 4.4% (range 1-57.9%). Absolute differences in VAF (tumor *vs.* nail) are depicted in Figure 2D, E; the distribution of individual events in tumor and corresponding nails are further detailed in Figure 3A-F. In 19 patients (0.7%; 19/2,610), nail mutations were detected at a VAF close to (<2-fold lower) or even slightly higher than those of the tumor sample, indicating high tumor contamination; details are provided in *Online Supplementary Table S3*. In three cases this could be attributed to gaps in collection, with nails collected at the time of highest disease burden and tumor at a very low level in a sample provided after interim therapy (Figure 3G). Despite the contamination, determination of somatic *versus* germline mutations was readily possible in all, except in a unique case represented in Figure 3H. Of note, among the myeloid neoplasms, mutations with the highest VAF in the tumor were more likely to be detected in the nail DNA. By contrast, among lymphoid neoplasms, mutated genes with the highest VAF in tumor were not detected in nail samples, supporting the concept that high tumor VAF alone does not drive the detection of mutations in the nail. The most commonly mutated genes in tumors and nails are depicted in Figure 4A, B. Mutations in nails were overwhelmingly biased to genes frequently altered in myeloid neoplasms in the spectrum of myeloproliferative neoplasms and myelodysplastic syndromes. While VAF in nails generally remained below 5%, alterations in *TET2, JAK2, ASXL1, DNMT3A, SRSF2* and *MPL* exhibited the highest number of outliers (Figure 4C). Prevalent pathological features across cases with mutations with VAF >5% (seen in 92 patients, 3.5% of the total cohort) included the presence of marked bone marrow fibrosis and osteosclerosis (33%, 31/92), and myeloid neoplasms with monocytic features (13%, 12/92). Mutations with the highest VAF also corresponded to genetic alterations with loss of heterozygosity. Representative cases are depicted in Figure 4D.

Notably, among the lymphoid and plasma cell neoplasms, common recurrent mutations in genes such as *BRAF, MYD88, IDH2, RHOA, IDH2, CREBBP, EP300* and others were distinctly absent in nails. Instead, 45% (53/118) of nail mutations overlapped with the most commonly described mutations in myeloid neoplasms. While a full work up was not possible in all cases, in selected patients (primarily those with nail mutations with VAF >3%), it could be determined that the patients had an emerging or coexisting clonal myeloid process with only mutations of myeloid origin identified in the nail. Selected case studies are depicted in Figure 5A-C. Among the patients with T-cell lymphomas and mutations in the nails, three had documented cutaneous involvement, together harboring 22 mutations, 32% of all

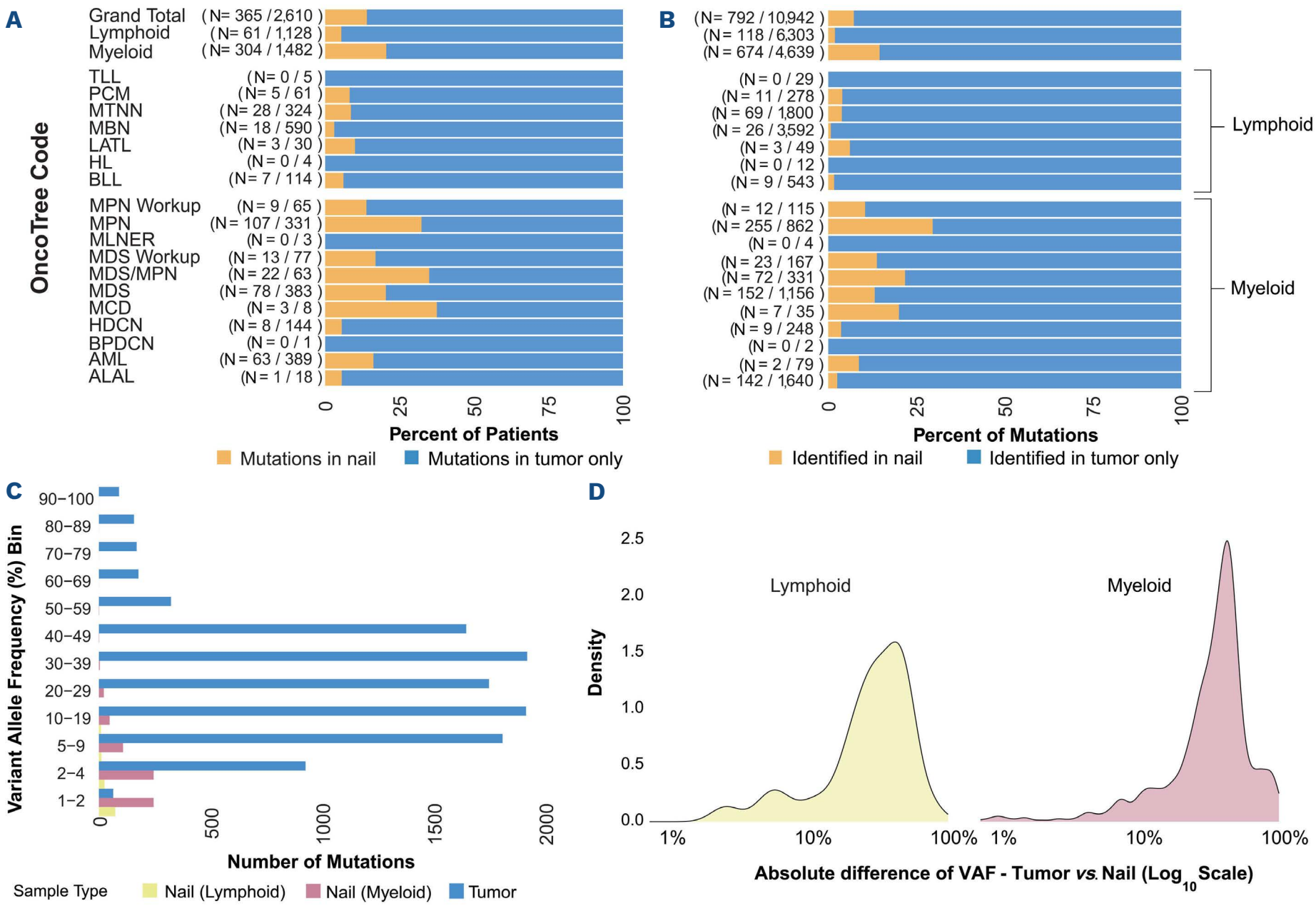

Figure 2. Distribution of patients and mutations by disease categories. (A) Distribution of patients in the clinical cohort. Patients are categorized by broad disease category (OncoTree Classification System) as specified on the far left (y axis). For each category, the number of patients is denoted inside the parentheses (N=patients with mutations in nail/total number of patients). The percent of patients is shown on the x axis. Yellow bars depict the proportion of patients with mutations in the nail; blue bars represent those patients with mutations identified only in tumor. The highest proportion of patients with mutations in the nail include those with mast cell disease, myelodysplastic/myeloproliferative neoplasms and myeloproliferative neoplasms. (B) Distribution of mutations in the clinical cohort. The number of mutations is categorized according to the same broad OncoTree categories as in (A). For each category, the number of mutations is specified inside the parentheses (N=mutations identified in nail/mutations in tumor only). The percent of mutations is depicted on the x axis. Yellow bars depict the proportion of mutations identified in the nail; blue bars correspond to mutations identified only in the tumor. Diseases with the highest proportion of mutations identified in the nail include myeloproliferative neoplasms, myelodysplastic/myeloproliferative neoplasms and mast cell disease. (C) Distribution of mutations by variant allele frequency (%), binned on the y axis, and number of mutations across the cohort on the x axis. Tumor mutations (blue bars) were distributed over a broad range with VAF averaging 26.7%. By contrast, mutations in nail were identified at significantly lower VAF ($P<2.2x10^{-16}$), average 4.4%. The VAF of mutations in nail were significantly lower for lymphoid neoplasms (yellow) compared to myeloid neoplasms (red), at 3.3% *versus* 4.9%, respectively ($P=0.006$). (D) Density plot depicting the absolute differences in VAF for mutations detected in the nail, compared to the same mutations in the corresponding tumor sample and stratified based on tumor category (Lymphoid *vs.* Myeloid). Mutations in nail are present at significantly lower VAF compared to the same mutation in the corresponding tumor. The large absolute differences between the tumor and the nail enables the determination that the variant is somatic in origin. The median absolute differences for mutations in patients with lymphoid malignancies was 29%, compared to 35% for those with myeloid malignancies. Using a non-parametric Wilcoxon rank sum test (Mann-Whitney U test), the differences in distribution of Lymphoid *versus* Myeloid are statistically significant ($P=0.0097$). Source data are provided as a Source Data file. TLL: T-lymphoblastic leukemia/lymphoma; PCM: plasma cell myeloma; MTNN: mature T and NK neoplasms; MBN: mature B-cell neoplasms; LATL: lymphoid atypical; HL: Hodgkin lymphoma; BLL: B-lymphoblastic leukemia/lymphoma; MPN Workup: cases with suspected MPN but for whom the work up was incomplete; MPN: myeloproliferative neoplasms; MLNER: myeloid/lymphoid neoplasms with eosinophilia and rearrangement of *PDGFRA/PDGFRB* or *FGFR1* or with *PCM1-JAK2*; MDS Workup: cases with suspected MDS but for whom the work up was incomplete; MDS/MPN: myelodysplastic/myeloproliferative neoplasms; MDS: myelodysplastic syndromes; MCD: mast cell diseases; HDCN: histiocytic and dendritic cell neoplasms; BPDCN: blastic plasmacytoid dendritic cell neoplasm; AML: acute myeloid leukemias; ALAL: acute leukemias of ambiguous lineage; VAF: variant allele frequency.

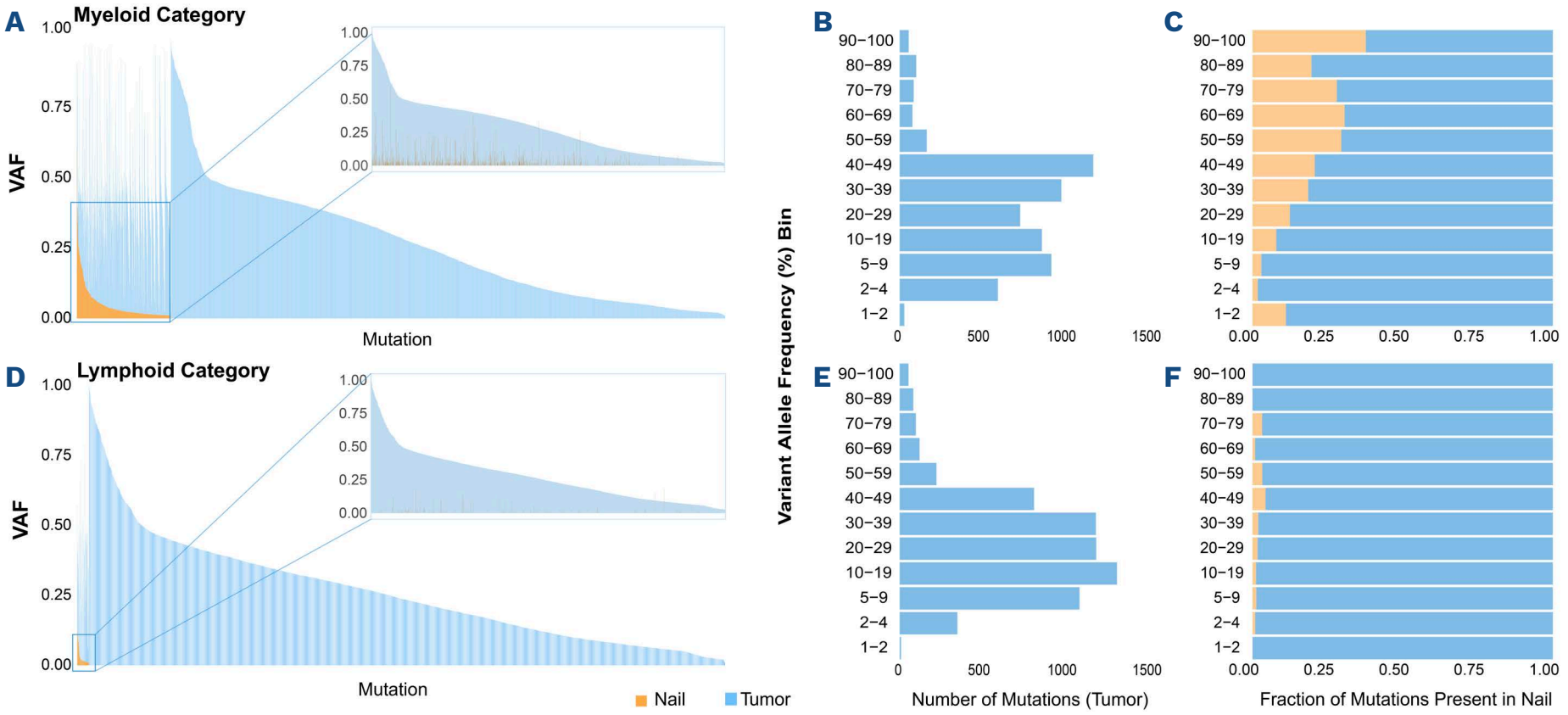

Gene	Mutation	VAF (%) Tumor	Nail (+120d)	Blood (+2yr)
JAK2	p.V617F	61.3	59.7	80.6
FBXO11	p.P45_Q53del	39.5	37.7	49.6
MGA	p.V2637L	36.2	27.4	46.4
ASXL1	p.W898*	19.3	19.3	34.6
ASXL1	p.R661*	10.2	8.8	3.1
FBXO11	p.D161Y	10.7	7.8	3.0
FANCD2	p.F386V	10.8	7.2	14.3

Figure 3. Comparison of variant allele frequencies between tumor DNA and nail DNA. (A-C) Distribution of mutations in patients with tumors in the myeloid category. (A) Bar graph depicting all mutations detected in the myeloid tumors (blue). Each bar represents one mutation. Nail DNA mutations (orange) are plotted next to the corresponding mutation in the tumor DNA. A total of 4,649 mutations were detected in the tumors. Of these, 674 (14.5%) were identified in the corresponding nails. Mutations in the nail are arranged by variant allele frequency (VAF) from highest to lowest (range, 1-59.7%). The subset of cases with nail mutations is expanded and reorganized by the corresponding VAF in the tumor, from highest to lowest, for comparison (zoomed area to the right). In all, 304 patients harbored the 674 mutations in the nail. Of these, 13 (4.3% of patients) had VAF > 20%. Despite tumor contamination in the nail, VAF in the nail were significantly lower than those in the tumor such that the distinction between somatic and germline variants could be made in all cases except in one patient (see details in 3H). Note that rare mutations are identified at slightly higher VAF in nail than in tumor. This corresponded to tumor samples submitted immediately after treatment, at the time of minimal residual disease, while the nail reflected contamination from several months previously when the level of disease was high level. (B) Mutations in myeloid tumors are stratified by their VAF (%) and binned as depicted on the y axis. The number of mutations in each category is denoted on the x axis. (C) The proportion of mutations identified in the nail based on the VAF of the mutation in the corresponding tumors. The VAF (%) of mutations in the tumor is shown on the y axis. The proportion of the corresponding mutations identified in the nail (orange) is given on the x axis. Note that in the myeloid category, the higher the VAF of the mutations in the tumor, the higher the proportion identified in the nail. (D-F) Distribution of mutations in patients with tumors in the lymphoid category. (D) Bar graph depicting all mutations detected in the lymphoid tumors (blue). Each bar represents one mutation. Nail mutations (orange) are plotted next to the corresponding mutation in the tumor. A total of 6,303 mutations were seen in the patients with lymphoid tumors. Of these, 118 mutations (1.9%) were identified in the corresponding nails. Mutations in the nail are arranged by VAF from highest to lowest (range, 1-17.4%). The set of cases with nail mutations is expanded and reorganized by the corresponding VAF in the tumor, from highest to lowest, for comparison (zoomed insert to the right). In all, 61 patients harbored the 118 mutations in the nail. (E) Mutations in lymphoid tumors are stratified by their VAF and binned as depicted on the y axis. The number of mutations in each category is denoted on the x axis. (F) The proportion of mutations identified in the nail based on the VAF of the mutation in the corresponding tumors. VAF (%) of mutations in the tumor is shown on the y axis. The proportion of the corresponding mutations identified in the nail (orange) is denoted on the x axis. Note that, in contrast to the myeloid tumors, mutations with the highest VAF in the tumor are not present in the nail. (G) Distribution of nail samples based on VAF and the timing of sampling relative to the corresponding tumor. The median interval between nail and tumor sampling was 3 days (range, 1,512 days before tumor sampling to 7,042 after tumor sam-

Continued on following page.

pling). The number of days is displayed on the x axis. Large gaps between collection of the two samples often reflected different disease loads causing diagnostic difficulties. (H) The only case in the cohort of 2,610 patients with mutations in the nail at a VAF of ~60% (similar to that of the tumor), raising the possibility of a germline event. Across the entire cohort, the highest VAF were associated with patients with myeloproliferative neoplasms and marked myelofibrosis. In all cases, except this unique case, the VAF in the tumor were comparatively higher (double), allowing discrimination of the mutation as somatic. In this case, the *JAK2* mutation was detected with a VAF of ~60% in both tumor and nail. According to the clinical history, this patient had occupational-related trauma to his hands and upper extremities. Multiple hematomas and ecchymoses on the upper extremities were documented in the weeks prior to the nail collection. The finding of several other mutations at high level and the overall pattern suggested tumor contamination, likely related to trauma. Reticulin staining of a prior bone marrow biopsy showed 3+ fibrosis. The table on the right lists all mutations and corresponding VAF in the tested blood sample, the corresponding nail collected 4 months later and the subsequent blood sample after 2 years.

mutations detected in the subset (22/69). Despite the high number of mutations, all were detected at a low level, with VAF between 1-2%.

Post-transplant nail samples

In all, 51 nail samples were collected after hematopoietic cell transplantation, at an average interval of 834 days (range, 3-3,918). Single nucleotide polymorphism profiles of tumor, donor and nail samples were compared to determine the presence of donor components in the nail. A subset (n=27) was also tested using standard short tandem repeat analysis for assessment of chimerism. The results are summarized in *Online Supplementary Table S4*. Of the 50 samples successfully analyzed, 78.3% (39/50) were 100% host and 22% (11/50) chimeric mostly host; the donor component ranged from 5 to 42%. There was no correlation between the presence and/or degree of donor component and the length of time since the transplant. In this cohort, a history of active graft-*versus*-host disease (within 5 months prior to nail sampling) was significantly more frequent among patients with donor DNA in the nail (63.6%; 7/11) compared to those with all host status (15.4%; 6/39) (*P*=0.001).

Discussion

Routine paired tumor-normal DNA sequencing has undeniable advantages in clinical genomics. This approach is ideal at many levels, not only for the unambiguous determination of somatic *versus* germline variants but also to facilitate the assessment of loss of heterozygosity and second hits in tumors, detect copy number alterations with higher sensitivity, estimate tumor mutation burden and mutational signatures more reliably, and to enable laboratory quality control checks related to sample identity. In previous studies we have shown that this can be successfully performed at a large scale in the clinical setting, both for solid[4,8,9] and liquid[1] tumors. The overall approach, however, proves to be more complex with hematologic malignancies, in which alternative sources of normal DNA must be explored. In this report, we concentrated on the use of nails as a unique source of DNA that is rarely utilized in clinical practice. To our knowledge, this is the largest and first study to describe its use for routine clinical comprehensive genomic testing.

The use of DNA from nails has been documented for over 30 years.[10-16] Historically, however, reports have remained scant and primarily confined to archeological, forensic, and epidemiological applications.[17-21] In the setting of cancer molecular diagnostics, our clinical laboratory has accumulated over 20 years of experience using nails for matched tumor:normal DNA testing.[22,23] Overall, while generally considered an excellent source of germline DNA, major limitations to the widespread use of nail clippings are related to the labor intensiveness of the extraction process and the scant/fragmented nature of the nucleic acid recovered. Biologically, nail DNA is a form of cell-free DNA (cfDNA) that originates from germinal matrix cells at the nail root.[24,25] During nail formation and growth, matrical cells mature and keratinize to ultimately form the structure of the nail plate. Through the keratinization phase, the cells undergo programed cell death and release fragmented DNA that remains embedded in the surrounding keratinous matrix. In contrast to cfDNA in body fluids, the water-free environment of nail matrix protects the DNA from rapid cytosine hydrolytic deamination damage or oxidant degradation, rendering it viable for decades.[26] Both the matrix and nail bed are highly vascularized, such that the nail plate may be influenced by, and incorporate, elements from the circulation.[27] Furthermore, fingernails take approximately 3-6 months in healthy patients to grow from the germinal matrix to the free edge and, therefore, the DNA captured from nail clippings constitutes a record of up to 6 months of previous growth, and may be longer in patients with underlying malignancy, poor nutritional state, and/or receiving anticancer therapies.

Several nail DNA extraction methods have been investigated in the past,[13,19] all involving cutting the nails into small fragments, followed by chemical lysis. Reported yields vary broadly, influenced by both biological and technical heterogeneity (size of the cut fragments, duration, and type of chemical lysis). Here, we outlined our optimized clinical extraction protocol, which incorporates mechanical bead pulverization. In addition to circumventing cumbersome cutting procedures, chemical digestion time is markedly reduced from days to hours, which is critical to enable testing in a clinically actionable time. With this new method,

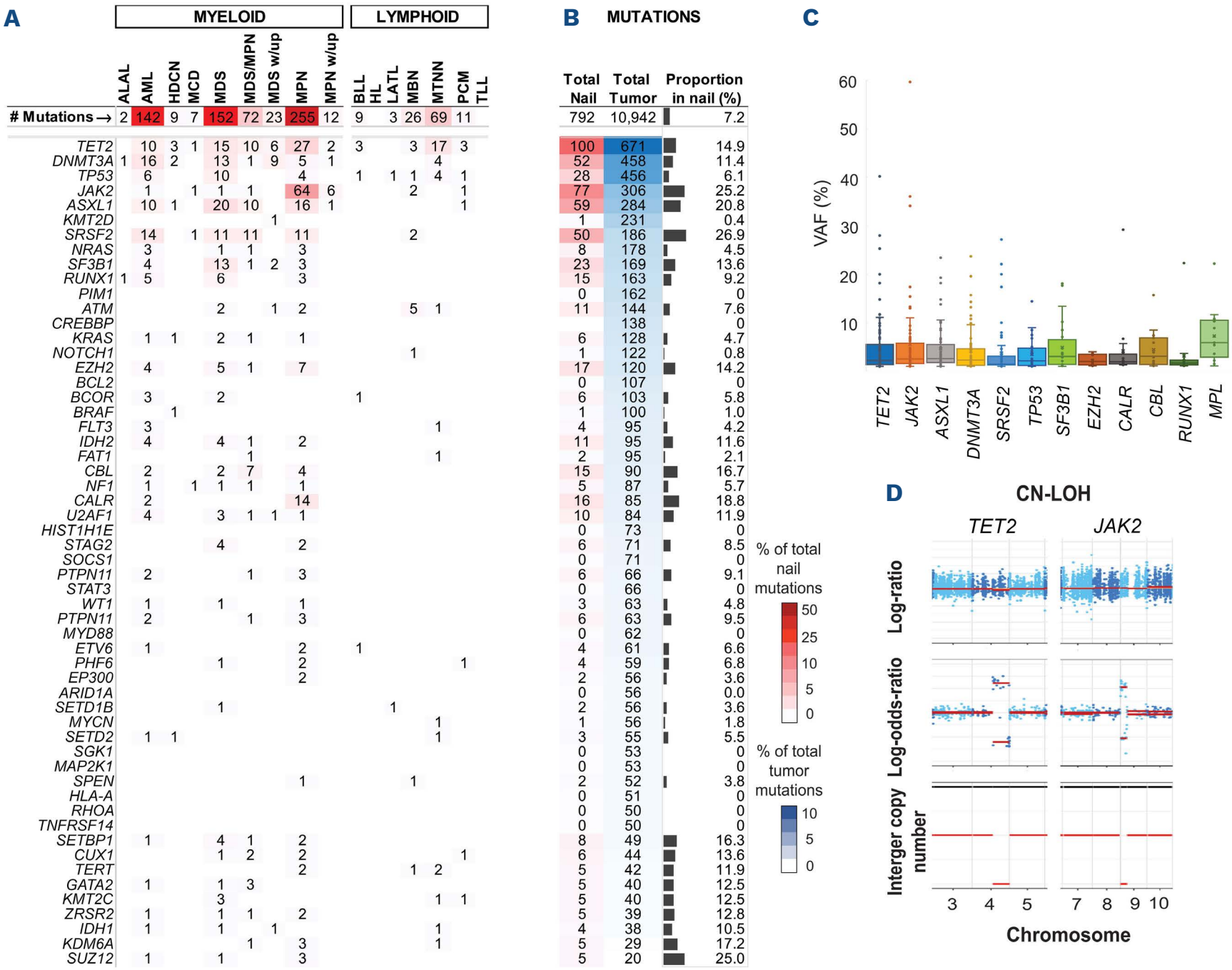

Figure 4. Most common alterations identified in nail DNA. (A) Heatmap showing the distribution of mutated genes identified in the nails based on disease categories. Genes included are the most commonly mutated, defined as those altered with a frequency >0.5% among the total mutations in nails or tumor. In nails, this encompassed genes mutated >4 times among the 792 mutations detected; in tumor, this encompassed genes mutated >50 times among the 10,942 mutations. Mutated genes are organized based on frequency in the tumor, with the highest number of mutations at the top. The total number of mutations in each disease category is annotated in the first row, followed by details of the number of mutations in each gene by disease category. Boxes are color coded as indicated by the color scale (red) indicating the percentage of total number of mutations identified in the nail. (B) The numbers of total mutations identified in each gene are listed in columns labeled Total Nail and Total Tumor. In the top row, all mutations detected in the cohort followed by detailed numbers for each gene. The proportions of total tumor mutations identified in the nail are displayed as percentages in the far-right column (plotted as a side bar and labeled). (C) Most frequently mutated genes in nails across all disease categories in order of frequency from left to right (*TET2* being most common). Distribution of mutations by variant allele frequency (VAF) (%) on the y axis. Although most mutations in these genes were identified in the nails at VAF <10%, these genes also had the highest number of outliers, often related to the presence of loss of heterozygosity (LOH). (D) Assessment of somatic copy number (CN) alteration profiles of two tumor samples demonstrate CN-LOH involving genes *TET2* (chromosome 4) and *JAK2* (chromosomes 9). MSK-IMPACT-heme analysis includes the assessment of genome-wide total and allele-specific copy number states which are calculated using the open-source R package FACETS2n (v0.3.0). The mutations were detected in the tumor at VAF of 91% (*TET2*) and 89% (*JAK2*), respectively. The corresponding nail samples had the same mutations at VAF of 40% and 36%, respectively. The figure shows the integrated visualization of FACETS analysis. The top panels display total CN log-ratio along genomic positions on chromosome 4 (left) and 9 (right), which are both copy neutral. The middle panels show the allele-specific log-odds-ratio revealing allelic divergence for regions of chromosomes 4 (left) and 9 (right), consistent with LOH events. The bottom panel displays the inferred integer CN with allelic losses of chromosomal segments 4 (left) and 9 (right) in the genomic regions containing *TET2* and *JAK2*, respectively (red lines). The black line corresponds to the total CN. ALAL: acute leukemias of ambiguous lineage; AML: acute myeloid leukemias; HDCN: histiocytic and dendritic cell neoplasms; MCD: mast cell diseases; MDS: myelodysplastic syndromes; MDS/MPN: myelodysplastic/myeloproliferative neoplasms; MDS w/up: cases with suspected MDS but for which work up was incomplete; MPN: myeloproliferative neoplasms; MPN w/up: cases with suspected MPN but for which work up was incomplete; BLL: B-lymphoblastic leukemia/lymphoma; HL: Hodgkin lymphoma; LATL: lymphoid atypical; MBN: mature B-cell neoplasms; MTNN: mature T and NK neoplasms; PCM: plasma cell myeloma; TLL: T-lymphoblastic leukemia/lymphoma.

A **CLL / SLL and Coexistent Myeloproliferative Neoplasm**

	1 Blood	2 Nail	3 BM	4 Sorted B	5 Sorted myeloid
KRAS G12D	3.7		5.5	4.4	
KRAS A146T	4.9		7.9	12.8	
NRAS G12A	1.3		2.0	3.0	
BRAF N581I	25.5		38.3	44.5	
MAP2K1 F53I	1.8		1.9	2.0	
ATM	5.4		18.8	24.9	
DDX3X	8.6		10.1	11.5	
DDX3X X500_splice	14.1		35.5	46.2	
JAK2 V617F	18.0	2.8	9.6		44.4
MPL W515L	8.2	1.0	4.0		35.6
FAT1 R3957H	9.2	2.0	4.9		24.1
NFE2 E261Afs*3	7.3	1.7	2.2		21.6
ESR1 S527N	2.0	1.0	1.0		14.6
TET2 H922Ifs*31					3.6

Bone marrow (3)

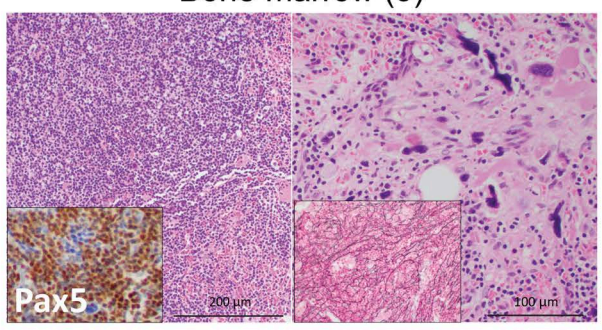

B **Plasma Cell Neoplasm and Emerging Myelodysplastic Syndrome**

	1 BM PCM	2 Nail	3 BM PCM & MDS (1yr)	4 Enriched PC	5 BM MDS (2yr)
MGAM S459F				17.8	
PHIP S1548C				13.8	
INPP4B G558*				2.7	
SET2D G2343*				2.3	
PCBP1 L100M				2.5	
KLF2 S263F				35.6	
CDH1 P126T				5.1	
SMC3 E955*				2.4	
SPEN G574W				5.3	
NOTCH1 G310W				2.1	
RAD21 R90W				36.0	
TP53 L330I				2.4	
KRAS Q22K				22.9	
PRDM1 R9H	2.6		5.7	52.8	
TET2 E1909Dfs*39	38.1	8.5	30.2		39.5
PHF6 X244_splice	33.4	8.5	34.8		38.2
TET2 L1398Hfs*2	34.7	8.7	29.3		38.0
CUX1 X654_splice	39.5	9.6	39.3		60.3
KMT2C R2139*	35.7	11.7	31.0		42.4

Bone marrow (3)

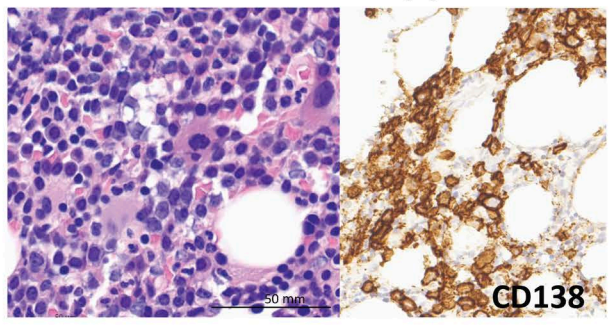

C **Angioimmunoblastic T-Cell Lymphoma and Evolving MDS/MPN**

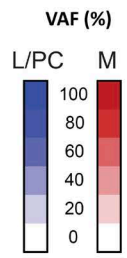

	1 Lymph node AITL	2 Nail	3 Blood (+6 mo)	4 BM (+1 yr)
HDAC4 G362A	15.4			
RHOA G17V	14.7			
IDH2 R172K	14.6			
CCND3 R271Pfs*53	13.4			
TET2 A379Vfs*6	11.5			
HGF S145G	9.0			
HLA-A X25_splice	7.6			
TET2 W1198*	45.2	18.2	81.8	79.2
DNMT3A Y724*	36.5	14.3	47.6	46.0
MYCN S369G	36.3	12.2	49.1	50.8
JAK2 V617F				38.0

Lymph node (1) Bone marrow (4)

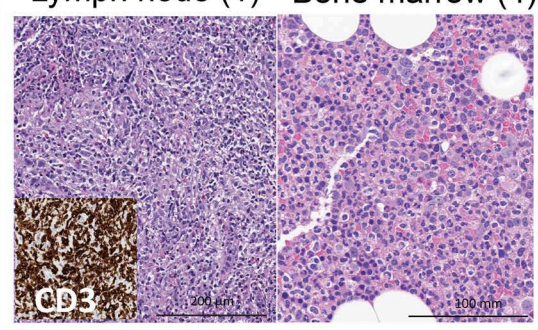

Figure 5. Representative cases of lymphoma or plasma cell neoplasms with tumor mutations identified in nail DNA. (A-C) The tables display the mutations detected in each sample sequenced, along with the corresponding variant allele frequencies (VAF) (%), highlighted according to the color scale (top right). Myeloid (M) lineage mutations are highlighted in red, lymphoid/plasma cell (L/PC)-associated mutations are highlighted in blue. Samples appear in order of collection; time in parenthesis is the interval relative to sample 1. (A) An 83-year-old male with a history of chronic lymphocytic leukemia/small lymphocytic lymphoma (CLL/SLL) for 13 years, on active surveillance (known *BRAF*, *NRAS* and *KRAS* mutations), presents for further assessment of suspected progression of disease (increased lymphocytosis, fatigue, anemia, and worsening thrombocytopenia). The blood sample (Bulk blood, 1) showed evidence of CLL/SLL, 59.4% by flow cytometry (FC). Sequencing revealed 13 mutations – the top eight were consistent with the previously diagnosed CLL/SLL. Other mutations (red) suggested a coexisting myeloproliferative neoplasm. Only the latter subset was detected in the nail (2). A bone marrow (BM) sample (3) was obtained 2 weeks later, demonstrating a genomic profile identical to that in the blood. B and myeloid cell populations were sorted (4 and 5, respectively) and sequenced independently, showing segregation of the mutations into two distinct categories of lymphoid and myeloid origin. Morphologically (bottom left), the BM sample revealed extensive CLL/SLL (insert highlights ~80% involvement by PAX-5 immunostain). At the bottom right there are areas with increased atypical megakaryocytes, severe reticulin fibrosis (insert shows retic stain), and no increase in blasts. The findings are consistent with a *JAK2* p.V617F and *MPL* p.W515L-mutated myeloproliferative neoplasm, fibrotic phase of primary myelofibrosis coexisting with CLL/SLL. Note that despite the known chronicity of the CLL and markedly higher VAF for the lymphoid-derived mutations, only myeloid-derived mutations are identified in the nail. (B) An 80-year-old female with a 2-year history of smoldering myeloma presents with progressive cytopenia. A BM sample was obtained (1) demonstrating patchy involvement by a plasma cell myeloma (PCM), ~15% by aspirate differential (2.9% of white blood cells by FC). No myelodysplasia was identified. Bulk BM sequencing revealed six mutations: one subclonal *PRDM1* and five mutations at high VAF (*TET2*, *PHF6*, *CUX1* and *KMT2C*), the latter five were also detected in the nail sample (2). A subsequent BM sample (3) 1 year later showed increased patchy involvement by PCM (40-80% on aspirate differential, 20% by FC) and overt dysplastic changes, while sequencing demonstrated the same mutations previously detected. To further assess the myeloma component, plasma cells (PC) were isolated from an aliquot of the same sample (CD138 magnetic bead-based positive selection) and sequenced (4). This enriched population established the myeloma-specific genomic profile, which excluded the five mutations detected in the nails. Further BM sampling 2 years later (5) showed overt multilineage dysplasia with a minimal PC component

Continued on following page.

(<5%). At this time the mutation profile reflected only the myeloid-derived mutations. The table displays the specific mutations detected in each sample. The bottom left picture depicts the findings of the BM sample (3), which is involved by both the PC neoplasm and myelodysplastic syndrome (MDS). Note the dysplastic megakaryocytes among numerous PC. CD138 immunostaining highlights the PC (bottom right). The overall findings are consistent with PC neoplasm with an emerging MDS. Mutations detected in the nail DNA correspond to those detected in the myeloid neoplasm and preceded overt morphological features of dysplasia. All PC lineage mutations were distinctly absent in the nail DNA. (C) A 71-year-old female with a history of angioimmunoblastic T-cell lymphoma (AITL) presented with disease recurrence. Sequencing of DNA from an involved lymph node showed the ten mutations detailed in the table (sample 1). Only a subset was detected in the nail DNA (2), specifically those associated with clonal hematopoiesis (CH) but hallmark mutations of AITL (*RHOA*, *IDH*) were distinctly absent. A blood sample (3) was obtained 6 months later, showing minimal involvement by an abnormal T-cell population (0.060% of the white blood cells by FC). However, sequencing demonstrated the same mutations (CH type) identified in the nail, at very high level. A follow up BM sample 1 year later demonstrated minimal residual involvement by AITL (0.0043% of white blood cells by FC); morphologically the BM was markedly hypercellular with mild dyspoiesis. Sequencing revealed the same three mutations and emergence of a *JAK2* mutation. In conjunction, the findings were consistent with a new myelodysplastic/myeloproliferative neoplasm (MDS/MPN) emerging in a patient with active AITL. The bottom left picture depicts the involvement by AITL in the lymph node (the insert shows cells highlighted by CD3 immunostaining). On the right, the markedly hypercellular BM can be seen.

average yields are also improved and above the highest reported, after adjusting for expected differences in DNA measurement methods.

We confirm that DNA recovered from nail tissue is highly fragmented, and in keeping with degraded cfDNA. This has specific implications for testing, posing limitations on methods that require long fragments. However, we find that the DNA performs very well in hybrid-capture-based NGS assays as well as polymerase chain reaction-based assays of short amplicons. In contrast to cfDNA from plasma, the insert size distribution of nail cfDNA exhibits a prominent jagged or sawtooth pattern with 10 bp periodicity. Similar findings were recently reported on sheared NGS libraries of five nail samples by Kakadia *et al.*[20] We postulate that this relates to specific and differential roles of DNases in nail tissue. In plasma, for instance, typical cfDNA fragment profiles primarily reflect the effect of DNAS1L3.[28] DNASE1 can further degrade DNA into shorter fragments with similar 10 bp periodicity, originating from digestion products of nucleosomes, which correspond to the 10 bp-per-turn structure of the DNA helix.[29] While this is not prominent in plasma, it is reported in urine in which DNASE1 activity is much higher.[30] In nail, degradation of endogenous DNA during cornification of keratinocytes is orchestrated by DNASE1L2[31] and may be responsible for this prominent pattern. Overall, the characteristic pattern suggests the protection of DNA from degradation by association with histones.

Our use of nail tissue in routine sequencing of hematologic malignancies highlighted important aspects of clinical utility that should be considered when implementing this control. One is that tumor contamination may be present in nail DNA in a small proportion of cases (13.9% in our cohort) and is distinctly biased toward the myeloid neoplasms. Importantly, in the overwhelming majority of cases, mutations were detected at low level, (98.5% at VAF <10% and 71.4% at VAF <2%) or at significantly lower VAF compared to that in the corresponding tumor, such that discrimination of the somatic *versus* germline nature of the variant was not compromised. Notably, VAF above 20% were rare, seen in 0.4% of patients (13/2,610), and over-represented in myeloproliferative neoplasms with extensive marrow myelofibrosis and osteosclerosis and which harbored mutations in genes affected by loss of heterozygosity. We hypothesize that, in this context, the high contribution of tumor DNA in nail arises from a high turn-over of circulating hematopoietic components in patients with extensive extramedullary hematopoiesis. The complications that occur in the natural history of patients with myelofibrosis, including both thrombotic and hemorrhagic events, may lead to entrapment of neoplastic cells in distal vascular locations, including the nail bed, where the DNA may become incorporated in the nail plate sampled. Contributing factors could also relate to adverse drug effects in skin and nail, such as hydroxyurea,[21] dietary factors and comorbidities.

While the causes of tumor DNA contamination in nail tissue remain to be defined, and are likely multifactorial in nature, the identification of the same common mutations across diseases, which also overlap with those seen in clonal hematopoiesis, could support the roles of inflammation, ongoing microvascular damage and increased risk of thrombo-hemorrhagic events as recently highlighted in numerous publications on clonal hematopoiesis.[32,33] For instance, commonly mutated genes in clonal hematopoiesis, acute myeloid leukemia, myelodysplastic syndromes and myeloproliferative neoplasms (*TET2, JAK2, ASXL1, DNMT3A, SF3B1* and *SH2B2*) have been associated with relative increases in platelet count and/or function and are implicated in the development of cardiovascular disease and thrombotic complications of both microvascular and macrovascular types.[34,35] Both thrombotic and hemorrhagic effects in the nail bed microvasculature could promote the release of tumor DNA as described above.

The relative paucity of nail mutations among patients with lymphoid neoplasms was unexpected, particularly in the context of T-cell lymphomas with cutaneous involvement. Mutations detected, and particularly those identified at VAF ≥2% (across B, T, and plasma cell neoplasms), were noteworthy for their overlapping profiles and frequent

association with synchronous or rapidly evolving myeloid neoplasms. In these cases, lymphoid-specific mutations were distinctly absent, serving as a discrete clue of a separate myeloid clonal process. It should be mentioned that, among T-cell lymphomas (particularly angioimmunoblastic T-cell lymphoma and T-follicular helper cell lymphoma), *TET2* and *DNMT3A* mutations are common alterations which can be shared across the T and myeloid compartments in approximately 70% of patients,[36-38] consistent with a common stem cell progenitor that may give rise to distinct neoplasms (~20%), highlighting prominent roles of clonal hematopoiesis in the development of both diseases. The presence of clonal hematopoiesis-type mutations across nail samples also raised the question of the role of chronicity and higher likelihood of tumor contamination due to extended exposure. While we cannot rule out a contribution, the presence of only clonal hematopoiesis-type mutations, even in largely chronic lymphoid neoplasms such as chronic lymphocytic leukemia/small cell lymphoma, would argue against this and seems to support a distinct biological behavior of these clonal populations.

Finally, the identification of donor DNA in nail clippings after allogeneic HCT has important implications for the use of nails as normal control material. Although literature remains scant, this finding has been previously documented. Results from two studies[39-41] (together 71 patients) have reported high variability in the incidence (43-100% of patients), proportion of donor component (4-95%) and even across fingernails of the same individual. While the reason remains unclear, possible mechanisms have been proposed which extrapolate from findings in other organ systems (donor cells in liver, lung, and others[42-44]), including donor hematopoietic stem cell conversion into non-hematopoietic cells and horizontal DNA transfer.[45-54] A potential etiology we also consider is graft-*versus*-host disease. While documented or overt findings in nails or skin were not consistently present on review of medical records, the higher incidence of the donor component among patients with a history of graft-*versus*-host disease within 5 months of sampling (the timeframe captured in a nail clipping) could support an active role and may reflect a systemic effect not necessarily evident on physical examination. Similar to what is seen among non-transplanted patients with myeloid neoplasms, mechanistically, it seems plausible that graft action on skin and distal vessels of the nail bed can lead to similar release of donor DNA that can be incorporated and detected in the clippings of the host nail plate. Further studies are required to better define this. Overall, however, and in the context of the central aspect of this work, it is important to qualify the suitability of the nail as a control by determining the presence and degree of chimerism. This may be done by short tandem repeat analysis prior to NGS testing. Alternatively, if the donor sample is also sequenced and the design of the assay allows, single nucleotide polymorphism analysis may also be performed. If there is minimal donor contamination, sequencing nail DNA in conjunction with the donor's DNA can be highly informative when analyzing data from difficult post-transplant samples.

In conclusion, in this report, we outline our experience using nail cfDNA as a "normal" control in comprehensive clinical genomic testing. While our findings support nail cfDNA as a highly valuable and informative source of DNA for paired studies, in a small subset of patients, nails reflect the patient's hematologic disease and transplant history. This should be considered as a possible limitation, but it could also be exploited as a potential diagnostic tool to inform undiagnosed disease. Through the analysis of our data and search of the limited literature available, it is evident that our understanding of key facets of the biology of nail and its interaction with the hematopoietic system remains poor, leaving many questions of practical and academic interest to be answered. Closer clinical and pathological assessment of nails in patients with hematologic diseases would enable further dedicated studies.

Disclosures

MK-W has been an advisory board member and speaker for AstraZeneca and has provided professional services for Foundation Medicine. KPD has received an honorarium (not related to this study) from Invivoscribe, Inc. RNP is an employee of C2i Genomics. RR has received consulting fees from Incyte Corporation, Celgene/BMS, Blueprint, AbbVie, CTI, Stemline, Galecto, Pharmaessentia, Constellation/Morphosys, Sierra Oncology/GSK, Cogent, Sumitomo Dainippon, Kartos, Servier, Zentalis, and Karyopharm and has received research funding from Constellation Pharmaceuticals, Ryvu, Zentalis, and Stemline Therapeutics. MAP reports honoraria from Adicet, Allogene, Allovir, Caribou Biosciences, Celgene, Bristol-Myers Squibb, Equilium, Exevir, ImmPACT Bio, Incyte, Karyopharm, Kite/Gilead, Merck, Miltenyi Biotec, MorphoSys, Nektar Therapeutics, Novartis, Omeros, OrcaBio, Sanofi, Syncopation, VectivBio AG, and Vor Biopharma; he serves on Data Safety Monitoring Boards for Cidara Therapeutics, Medigene, and Sellas Life Sciences, and on a scientific advisory board of NexImmune; he has ownership interests in NexImmune, Omeros, and OrcaBio; and has received institutional research support for clinical trials from Allogene, Incyte, Kite/Gilead, Miltenyi Biotec, Nektar Therapeutics, and Novartis. SH is a consultant for Affimed, Abcuro Inc, Corvus, Daiichi Sankyo, Kyowa Hakko Kirin, ONO Pharmaceuticals, SeaGen, SecuraBio, Takeda, and Yingli; and has received research support from ADC Therapeutics, Affimed, C4, Celgene, Crispr Therapeutics, Daiichi Sankyo, Dren Kyowa Hakko Kirin, Millennium/Takeda, Seattle Genetics, and SecuraBio. DP has received honoraria from Incyte and Sanofi; has served on advisory boards for Evive Biotechnology (Shanghai) Ltd (formerly Generon [Shanghai] Corporation Ltd), Kadmon-Sanofi Corporation, Ceramedix, and Incyte; and has received research fund-

ing from Incyte Corporation and Sanofi. AM has received research funding from AstraZeneca, Incyte Corporation, Kintara Therapeutics, and Amryt Pharma; has provided consultancy services for ADC Therapeutics, Alira Health, AstraZeneca, Protagonist Therapeutics, OnQuality, and Janssen; and has received royalties from UpToDate. SM is the principal owner of Daboia Consulting LLC. AD receives research support from Roche and Takeda. MFB has provided consultancy services for Eli Lilly, AstraZeneca, and Paige.AI; has received research support from Boundless Bio; and has intellectual property rights with SOPHiA Genetics. CV holds equity and intellectual property rights with, and provides professional services and activities for Paige.AI. MEA has acted as a speaker for Biocartis, Invivoscribe, Physician Educational Resources (PER), Peerview Institute for Medical Education, Clinical Care Options, and RMEI Medical Education; and has acted as a consultant for Janssen Global Services, Bristol-Myers Squibb, AstraZeneca, Roche, Biocartis, and Sanofi.

Contributions

MEA, CV, RP, MFB, and MK-W reviewed, analyzed, and interpreted data, performed the statistical analyses and drew conclusions. All authors read and reviewed the manuscript and contributed to the review process.

Funding

This study at Memorial Sloan Kettering Cancer Center was supported by Comprehensive Cancer Center Core grant P30CA008748 from the National Institutes of Health.

Data-sharing statement

The minimal clinical and somatic alteration data (including mutations and allele-specific copy number calls) necessary to replicate the findings in the article have been deposited at https://github.com/chadvanderbilt/Nails/tree/main/data. Source data are provided. Raw sequencing data cannot be broadly available due to privacy laws; patients' consent to deposit raw sequencing data was not obtained.

References

1. Ptashkin RN, Ewalt MD, Jayakumaran G, et al. Enhanced clinical assessment of hematologic malignancies through routine paired tumor and normal sequencing. Nat Commun. 2023;14(1):6895.
2. Kontopoulos I, Penkman K, Mullin VE, et al. Screening archaeological bone for palaeogenetic and palaeoproteomic studies. PLoS One. 2020;15(6):e0235146.
3. Kontopoulos I, Presslee S, Penkman K, Collins M. Preparation of bone powder for FTIR-ATR analysis: the particle size effect. Vibr Spectrosc. 2018;99:167-177.
4. Zehir A, Benayed R, Shah RH, et al. Mutational landscape of metastatic cancer revealed from prospective clinical sequencing of 10,000 patients. Nat Med. 2017;23(6):703-713.
5. Cheng DT, Mitchell TN, Zehir A, et al. Memorial Sloan Kettering-Integrated Mutation Profiling of Actionable Cancer Targets (MSK-IMPACT): a hybridization capture-based next-generation sequencing clinical assay for solid tumor molecular oncology. J Mol Diagn. 2015;17(3):251-264.
6. Shen R, Seshan VE. FACETS: allele-specific copy number and clonal heterogeneity analysis tool for high-throughput DNA sequencing. Nucleic Acids Res. 2016;44(16):e131.
7. Chakravarty D, Gao J, Phillips SM, et al. OncoKB: a precision oncology knowledge base. JCO Precis Oncol. 2017;2017:PO.17.00011.
8. Frampton GM, Fichtenholtz A, Otto GA, et al. Development and validation of a clinical cancer genomic profiling test based on massively parallel DNA sequencing. Nat Biotechnol. 2013;31(11):1023-1031.
9. Wagle N, Berger MF, Davis MJ, et al. High-throughput detection of actionable genomic alterations in clinical tumor samples by targeted, massively parallel sequencing. Cancer Discov. 2012;2(1):82-93.
10. Berglund EC, Kiialainen A, Syvänen AC. Next-generation sequencing technologies and applications for human genetic history and forensics. Investig Genet. 2011;2:23.
11. Krskova-Honzatkova L, Sieglova Z. Fingernail DNA: a suitable source of constitutional DNA in leukemia. Lab Hematol. 2000;6:145-146.
12. Matsuzawa N, Shimozato K, Natsume N, Niikawa N, Yoshiura K. A novel missense mutation in Van der Woude syndrome: usefulness of fingernail DNA for genetic analysis. J Dent Res. 2006;85(12):1143-1146.
13. Nakashima M, Tsuda M, Kinoshita A, et al. Precision of high-throughput single-nucleotide polymorphism genotyping with fingernail DNA: comparison with blood DNA. Clin Chem. 2008;54(10):1746-1748.
14. Park J, Liang D, Kim JW, et al. Nail DNA and possible biomarkers: a pilot study. J Prev Med Public Health. 2012;45(4):235-243.
15. Tanigawara Y, Kita T, Hirono M, Sakaeda T, Komada F, Okumura K. Identification of N-acetyltransferase 2 and CYP2C19 genotypes for hair, buccal cell swabs, or fingernails compared with blood. Ther Drug Monit. 2001;23(4):341-346.
16. van Breda SG, Hogervorst JG, Schouten LJ, et al. Toenails: an easily accessible and long-term stable source of DNA for genetic analyses in large-scale epidemiological studies. Clin Chem. 2007;53(6):1168-1170.
17. Hogervorst JG, Godschalk RW, van den Brandt PA, et al. DNA from nails for genetic analyses in large-scale epidemiologic studies. Cancer Epidemiol Biomarkers Prev. 2014;23(12):2703-2712.
18. Truong L, Park HL, Chang SS, et al. Human nail clippings as a source of DNA for genetic studies. Open J Epidemiol. 2015;5(1):41-50.
19. Preuner S, Danzer M, Pröll J, et al. High-quality DNA from fingernails for genetic analysis. J Mol Diagn. 2014;16(4):459-466.
20. Kakadia PM, Van de Water N, Browett PJ, Bohlander SK. Efficient identification of somatic mutations in acute myeloid leukaemia

using whole exome sequencing of fingernail derived DNA as germline control. Sci Rep. 2018;8(1):13751.
21. Malato A, Rossi E, Palumbo GA, Guglielmelli P, Pugliese N. Drug-related cutaneous adverse events in Philadelphia chromosome-negative myeloproliferative neoplasms: a literature review. Int J Mol Sci. 2020;21(11):3900.
22. Barbashina V, Salazar P, Holland EC, Rosenblum MK, Ladanyi M. Allelic losses at 1p36 and 19q13 in gliomas: correlation with histologic classification, definition of a 150-kb minimal deleted region on 1p36, and evaluation of CAMTA1 as a candidate tumor suppressor gene. Clin Cancer Res. 2005;11(3):1119-1128.
23. Barbashina V, Salazar P, Ladanyi M, Rosenblum MK, Edgar MA. Glioneuronal tumor with neuropil-like islands (GTNI): a report of 8 cases with chromosome 1p/19q deletion analysis. Am J Surg Pathol. 2007;31(8):1196-1202.
24. Eckhart L, Lippens S, Tschachler E, Declercq W. Cell death by cornification. Biochim Biophys Acta. 2013;1833(12):3471-3480.
25. de Berker DA, André J, Baran R. Nail biology and nail science. Int J Cosmet Sci. 2007;29(4):241-275.
26. Bengtsson CF, Olsen ME, Brandt L, et al. DNA from keratinous tissue. Part I: hair and nail. Ann Anat. 2012;194(1):17-25.
27. de Berker D. Nail anatomy. Clin Dermatol. 2013;31(5):509-515.
28. Han DSC, Ni M, Chan RWY, et al. The biology of cell-free DNA fragmentation and the roles of DNASE1, DNASE1L3, and DFFB. Am J Hum Genet. 2020;106(2):202-214.
29. Klug A, Lutter LC. The helical periodicity of DNA on the nucleosome. Nucleic Acids Res. 1981;9(17):4267-4283.
30. Xie T, Wang G, Ding SC, et al. High-resolution analysis for urinary DNA jagged ends. NPJ Genom Med. 2022;7(1):14.
31. Fischer H, Scherz J, Szabo S, et al. DNase 2 is the main DNA-degrading enzyme of the stratum corneum. PLoS One. 2011;6(3):e17581.
32. Avagyan S, Zon LI. Clonal hematopoiesis and inflammation - the perpetual cycle. Trends Cell Biol. 2023;33(8):695-707.
33. Marnell CS, Bick A, Natarajan P. Clonal hematopoiesis of indeterminate potential (CHIP): linking somatic mutations, hematopoiesis, chronic inflammation and cardiovascular disease. J Mol Cell Cardiol. 2021;161:98-105.
34. Olivi M, Di Biase F, Lanzarone G, et al. Thrombosis in acute myeloid leukemia: pathogenesis, risk factors and therapeutic challenges. Curr Treat Options Oncol. 2023;24(6):693-710.
35. Papageorgiou L, Elalamy I, Vandreden P, Gerotziafas GT. Thrombotic and hemorrhagic issues associated with myeloproliferative neoplasms. Clin Appl Thromb Hemost. 2022;28:10760296221097969.
36. Lewis NE, Petrova-Drus K, Huet S, et al. Clonal hematopoiesis in angioimmunoblastic T-cell lymphoma with divergent evolution to myeloid neoplasms. Blood Adv. 2020;4(10):2261-2271.
37. Nann D, Fend F, Quintanilla-Martinez L. [TFH lymphoma and associated clonal hematopoiesis]. Pathologie (Heidelb). 2023;44(Suppl 3):144-149.
38. Cheng S, Zhang W, Inghirami G, Tam W. Mutation analysis links angioimmunoblastic T-cell lymphoma to clonal hematopoiesis and smoking. Elife. 2021;10:e66395.
39. Imanishi D, Miyazaki Y, Yamasaki R, et al. Donor-derived DNA in fingernails among recipients of allogeneic hematopoietic stem-cell transplants. Blood. 2007;110(7):2231-2234.
40. Sanz-Piña E, Santurtún A, Freire J, Gómez-Román J, Colorado M, Zarrabeitia MT. The genetic profile of bone marrow transplant patients in different samples of forensic interest. Forensic Sci Med Pathol. 2019;15(2):178-183.
41. Robesova B, Drncova M, Folta A, et al. Donor-derived DNA variability in fingernails of acute myeloid leukemia patients after allogeneic hematopoietic stem cell transplantation detected by direct PCR. Bone Marrow Transplant. 2020;55(6):1021-1022.
42. Suratt BT, Cool CD, Serls AE, et al. Human pulmonary chimerism after hematopoietic stem cell transplantation. Am J Respir Crit Care Med. 2003;168(3):318-322.
43. Alison MR, Poulsom R, Jeffery R, et al. Hepatocytes from non-hepatic adult stem cells. Nature. 2000;406(6793):257.
44. Bittner RE, Schöfer C, Weipoltshammer K, et al. Recruitment of bone-marrow-derived cells by skeletal and cardiac muscle in adult dystrophic mdx mice. Anat Embryol (Berl). 1999;199(5):391-396.
45. Waterhouse M, Themeli M, Bertz H, Zoumbos N, Finke J, Spyridonidis A. Horizontal DNA transfer from donor to host cells as an alternative mechanism of epithelial chimerism after allogeneic hematopoietic cell transplantation. Biol Blood Marrow Transplant. 2011;17(3):319-329.
46. Jang YY, Collector MI, Baylin SB, Diehl AM, Sharkis SJ. Hematopoietic stem cells convert into liver cells within days without fusion. Nat Cell Biol. 2004;6(6):532-539.
47. Terada N, Hamazaki T, Oka M, et al. Bone marrow cells adopt the phenotype of other cells by spontaneous cell fusion. Nature. 2002;416(6880):542-545.
48. Metaxas Y, Zeiser R, Schmitt-Graeff A, et al. Human hematopoietic cell transplantation results in generation of donor-derived epithelial cells. Leukemia. 2005;19(7):1287-1289.
49. Spyridonidis A, Schmitt-Gräff A, Tomann T, et al. Epithelial tissue chimerism after human hematopoietic cell transplantation is a real phenomenon. Am J Pathol. 2004;164(4):1147-1155.
50. Tran SD, Pillemer SR, Dutra A, et al. Differentiation of human bone marrow-derived cells into buccal epithelial cells in vivo: a molecular analytical study. Lancet. 2003;361(9363):1084-1088.
51. Spyridonidis A, Zeiser R, Follo M, Metaxas Y, Finke J. Stem cell plasticity: the debate begins to clarify. Stem Cell Rev. 2005;1(1):37-43.
52. Jiang Y, Jahagirdar BN, Reinhardt RL, et al. Pluripotency of mesenchymal stem cells derived from adult marrow. Nature. 2002;418(6893):41-49.
53. Takahashi K, Yamanaka S. Induction of pluripotent stem cells from mouse embryonic and adult fibroblast cultures by defined factors. Cell. 2006;126(4):663-676.
54. Halicka HD, Bedner E, Darzynkiewicz Z. Segregation of RNA and separate packaging of DNA and RNA in apoptotic bodies during apoptosis. Exp Cell Res. 2000;260(2):248-256.